Monthly Notices of the ROYAL ASTRONOMICAL SOCIETY

MNRAS **453,** 106–112 (2015) doi:10.1093/mnras/stv1583

Binary open clusters in the Milky Way: photometric and spectroscopic analysis of NGC 5617 and Trumpler 22

G. M. De Silva,[1,2★] G. Carraro,[3,4] V. D'Orazi,[5,6,7] V. Efremova,[1] H. Macpherson,[1,6] S. Martell[8] and L. Rizzo[9]

[1]*Australian Astronomical Observatory, 105 Delhi Rd, NSW 2113, Australia*
[2]*Sydney Institute for Astronomy, School of Physics, The University of Sydney, NSW 2006, Australia*
[3]*ESO, Alonso de Cordova 3107, 19001 Santiago de Chile, Chile*
[4]*Dipartimento di Astronomia e Fisica, Universita di Padova, Vicolo dell'Osservatorio 3, I-35122 Padova, Italy*
[5]*INAF – Osservatorio Astronomico di Padova, vicolo dell'Osservatorio 5, I-35122 Padova, Italy*
[6]*Monash Center for Astrophysics, School of Physics and Astronomy, Monash University, VIC 3800, Australia*
[7]*Department of Physics and Astronomy, Macquarie University, North Ryde, NSW 2109, Australia*
[8]*School of Physics, University of New South Wales, Sydney, NSW 2052, Australia*
[9]*Facultad de Ciencias Astronómicas y Geofísicas (UNLP), Universidad de La Plata (CONICET, UNLP), Paseo del Bosque s/n, La Plata 1900, Argentina*

Accepted 2015 July 12. Received 2015 July 12; in original form 2015 May 5

ABSTRACT

Using photometry and high-resolution spectroscopy we investigate for the first time the physical connection between the open clusters NGC 5617 and Trumpler 22. Based on new CCD photometry we report their spatial proximity and common age of ∼70 Myr. Based on high-resolution spectra collected using the HERMES and UCLES spectrographs on the Anglo-Australian telescope, we present radial velocities and abundances for Fe, Na, Mg, Al, Si, Ca, and Ni. The measured radial velocities are -38.63 ± 2.25 km s^{-1} for NGC 5617 and -38.46 ± 2.08 km s^{-1} for Trumpler 22. The mean metallicity of NGC 5617 was found to be [Fe/H] $= -0.18 \pm 0.02$ and for Trumpler 22 was found to be [Fe/H] $= -0.17 \pm 0.04$. The two clusters share similar abundances across the other elements, indicative of a common chemical enrichment history of these clusters. Together with common motions and ages we confirm that NGC 5617 and Trumpler 22 are a primordial binary cluster pair in the Milky Way.

Key words: open clusters and associations: general – open clusters and associations: individual: NGC 5617 – open clusters and associations: individual: Trumpler 22.

1 INTRODUCTION

The current model of the global star formation hierarchy is that giant molecular clouds fragment into cloud cores, producing stellar complexes, OB associations and open clusters which dissipate into individual stars (Efremov 1995). The exact mechanism that lead from the contraction of molecular clouds to star clusters is not completely understood, and likely there are different paths that lead to the formation of different systems of clusters. In the later stages of this hierarchy, it has been suggested that star clusters could form in pairs or multiples (de la Fuente Marcos & de la Fuente Marcos 2009). We refer to such clusters as primordial binary clusters.

Primordial binary clusters are expected to be transient in nature, where possible subsequent evolutionary paths include merging of the pair, tidal disruption of one or both clusters, and separation into two bound clusters. The models of Bhatia (1990) suggest that binary cluster lifetimes range from a few 10^6 yr to 4×10^7 yr depending on factors such as cluster separation, tidal force of the parental galaxy and encounters with giant molecular clouds. The identification of primordial binary clusters is further complicated with possible other explanations for their origins. The mechanisms of tidal capture and resonant trapping can place two unrelated clusters in pairs (Leon, Bergond & Vallenari 1999), and these tend to eventually merge (de Oliveira, Bica & Dottori 2000b; de Oliveira et al. 2000a). Some candidate binary clusters could be merely optical doubles due to superpositioning along the field of view.

In the Large and Small Magellanic Clouds (LMC and SMC), at least 10 per cent of the known open cluster systems may be in pairs and perhaps more than 50 per cent of these are primordial binary clusters (Bhatia & Hatzidimitriou 1988; Dieball & Grebel 2000; Dieball, Müller & Grebel 2002). Interaction between the LMC and the SMC may be the conditions giving rise to the formation of primordial binary star clusters (Fujimoto & Kumai 1997). Binary and multiple star clusters have been seen in other violent environments including in the Antennae galaxies (Fall, Chandar & Whitmore

★ E-mail: gayandhi.desilva@aao.gov.au

2005; Whitmore et al. 2005) and in the young starburst galaxy M51 (Larsen 2000; Bastian et al. 2005), presumably initiated by galaxy–galaxy interactions. The merger of large binary cluster systems has been suggested to lead to the formation of massive globular clusters, such as Omega Cen (Minniti et al. 2004) and NGC 1851 (Carretta et al. 2010).

In the Milky Way 10 per cent of the Galactic open clusters have been proposed to be in binary or multiple systems (e.g. Subramaniam et al. 1995; de la Fuente Marcos & de la Fuente Marcos 2010). The most well established binary cluster in the Galaxy is the pair *h* and χ Persei (Dufton et al. 1990; Marco & Bernabeu 2001; Uribe et al. 2002). None of the other proposed binary candidates have been verified with spectroscopic studies. Kopchev & Petrov (2008) studied the binary candidate pair NGC 7031/NGC 7086 and based on photometry, found a discrepancy in age, which may be due to large age uncertainties, and encouraged radial velocity follow-up. Vázquez et al. (2010) searched for candidate binary clusters in the 3rd Galactic Quadrant with a negative outcome and concluded binary clusters would form preferentially in environments closer to the environment of the LMC, suggesting further investigations in denser and more violent regions of the Milky Way, such as the inner Galaxy.

The apparent lack of confirmed binary or multiple open clusters in the Galaxy leads to several questions. Did the Milky Way not undergo a violent past to form such structures? If it did, perhaps the time-scales have been too short to preserve any binary clusters today, as the transient nature of binary clusters meant they are no longer in existence as a binary system. Or have we not looked hard enough for binary clusters in our own Galaxy?

A possible tracer of cluster origins is the motion and chemical abundance composition of their stars. Presumably if two clusters formed at about the same time and site, then they should have similar ages, motions, and chemical properties, assuming that the larger gas cloud was sufficiently mixed, with no major contamination events (e.g. supernovae) taking place during the cluster formation time-scales. As the chemical abundance patterns in low-mass stars are preserved during their lives, they reflect the conditions of their birth site. Hence a pair of primordial binaries should share a common age, radial velocity, and chemical composition. Binary clusters caused by tidal capture may show common motion, but the chemical properties and ages are likely to be different. For any optical doubles we expect both the motion and chemical composition to be different between the two clusters.

In this paper we present the first spectroscopic study of stars in the binary open cluster pair Trumpler 22 and NGC 5617. They are a strong primordial binary candidate with estimated ages of 70 ± 10 Myr (this study) and the pair are spatially separated by only 20 pc (Subramaniam et al. 1995). Stellar membership has been explored in the literature for NGC 5617 (e.g. Carraro & Munari 2004; Ahumada 2005; Frinchaboy & Majewski 2008; Mermilliod, Mayor & Udry 2008; Orsatti et al. 2010; Carraro 2011); however, very few studies have targeted Trumpler 22. This paper is organized as follows: Section 2 presents the photometric data on the target cluster which also formed the selection criteria for the subsequent spectroscopic observations. In Section 3, we present the radial velocity analysis. In Section 4, we discuss the spectroscopic analysis. The findings are summarized in Section 5.

2 PHOTOMETRY

The photometry used in this paper comes from two sources. In the case of NGC 5617, modern CCD photometry in the *UBVI* passbands is available from Carraro (2011). In this study, estimates of the cluster fundamental parameters are derived. The age is constrained to 70 ± 10 Myr, while the distance from the Sun is 2.1 ± 0.2 kpc, and the reddening $E(B-V) = 0.45 \pm 0.05$. According to this study, the reddening law in the line of sight is normal ($R_V = 3.1$).

Table 1. *UBVI* photometric observations of Trumpler 22 and Landolt standard stars on 2011 June 3.

Field	Filter	Exposures (s)	Airmass (X)
Trumpler 22	*U*	30, 2 × 180, 900	1.07–1.28
	B	10, 2 × 120,600	1.07 –1.27
	V	5, 2 × 60, 300	1.07–1.27
	I	5, 2 × 60, 300	1.07–1.26
PG1323	*U*	4 × 240	1.17–2.05
	B	4 × 120	1.18–2.00
	V	4 × 60	1.18–2.05
	I	4 × 60	1.20–2.10
PG16333	*U*	4 × 240	1.17–1.87
	B	4 × 120	1.18–1.95
	V	4 × 60	1.18–1.92
	I	4 × 60	1.20–1.88
Mark A	*U*	4 × 240	1.03–1.57
	B	4 × 120	1.03–1.55
	V	4 × 60	1.03–1.54
	I	4 × 60	1.03–1.56

For Trumpler 22, only old photographic data exist (Haug 1978), and for this reason we exploit here a new data set. Photometry in *UBVI* was acquired at Las Campanas Observatory on the nights from 2011 June 03 and are published here for the first time. We used the SITe#3 CCD detector onboard the Swope 1.0 m telescope.[1] With a pixel scale of 0.435 arcsec pixel^{-1}, this CCD allows us to cover 14.8 arcmin × 22.8 arcmin on sky. We stress that this setup (telescope/instrument) is the same that Carraro (2011) used for NGC 5617. The night was photometric with seeing ranging from 0.8 to 1.5 arcsec. We obtained multiple exposures per filter, and observed three times along the night the standard star field PG 1323, Mark A, and PG 1633, to cover a wide airmass range, and to secure proper photometric calibration (see Table 1). After removing problematic stars, and stars having only a few observations in Landolt's (1992) catalogue, our photometric solution for the run was extracted from a grand total of 63 measurements per filter, and turned out to be:

$$U = u + (5.004 \pm 0.010) + (0.49 \pm 0.010) \times X + (0.129 \pm 0.013) \times (U - B)$$
$$B = b + (3.283 \pm 0.006) + (0.25 \pm 0.010) \times X + (0.040 \pm 0.008) \times (B - V)$$
$$V = v + (3.204 \pm 0.005) + (0.16 \pm 0.010) \times X - (0.066 \pm 0.008) \times (B - V)$$
$$I = i + (3.508 \pm 0.005) + (0.08 \pm 0.010) \times X + (0.037 \pm 0.006) \times (V - I),$$

where *X* indicates the airmass.

After standard pre-processing, photometry was extracted using the DAOPHOT/ALLFRAME package (Stetson 1987). The photometry data set has finally astrometrized using the 2MASS[2] catalogue. The data will be made available at the SIMBAD Astronomical Database.[3]

We compared our photometry with (Haug 1978) photographic photometry for 65 stars in common. The comparison reads:

[1] http://www.lco.cl/telescopes-information/henrietta-swope/
[2] http://www.ipac.caltech.edu/2mass/
[3] http://simbad.u-strasbg.fr/simbad/

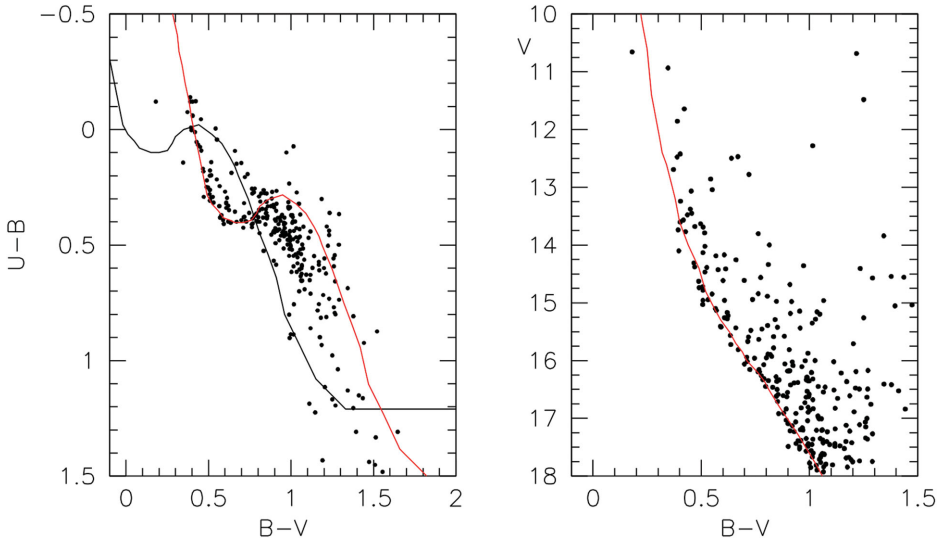

Figure 1. Left-hand panel: colour–colour diagram for Trumpler 22 stars within 4 arcmin from the cluster nominal centre. The solid lines are zero-age main-sequence relations for no-reddening (black line) and for $E(B-V) = 0.48$ (red line). This latter line nicely fits the bulk of early-type stars. Right-hand panel: colour–magnitude diagram for the same stars as in the left-hand panel. The solid line has been displaced horizontally, by $E(B-V) = 0.48$, and, vertically, by $(m-M) = 13.10$.

$\delta V = -0.05 \pm 0.12$, $\delta(B-V) = -0.09 \pm 0.11$, and $\delta(U-B) = -0.11 \pm 0.20$, in the direction of our photometry minus (Haug 1978). Such systematic differences are not worrisome, and can be explained by small zero-points differences caused by the use of different telescopes, and different techniques (variable PSF versus fixed aperture diaphragm).

In Fig. 1 (left-hand panel), we show the colour-color diagram (CCD), that we used to estimate the cluster reddening, while in the right-hand panel we shown Trumpler 22 colour–magnitude diagram (CMD), used to estimate the distance. Only stars within 4 arcmin from the cluster nominal centre are plotted. The reddening is estimated by displacing an empirical zero-age main sequence (ZAMS; Schmidt-Kaler 1982) along the reddening line. The un-reddened ZAMS is shown as a black line, while the red line is the same ZAMS, shifted by $E(B-V) = 0.48 \pm 0.08$. The sequence of early-type stars is tight enough to assume we are facing a real cluster. In the right-hand panel, the same sample of stars is fitted with a ZAMS for the same reddening and for an apparent distance modulus $(m-M) = 13.1 \pm 0.2$. Both reddening, distance modulus, and the associated uncertainties have been estimated via the usual visual inspection method.

This implies a distance of 2.10 ± 0.3 kpc, and we conclude that Trumpler 22 and NGC 5617 share the same heliocentric distance.

To estimate the age of Trumpler 22, we constructed the reddening-corrected CMD for the star within 4 arcmin form the centre in Fig. 2. In this diagram, Trumpler 22 stars are indicated with red circles. Black circles are stars from NGC 5617, corrected for reddening as well. One can readily notice that the two clusters lie nicely one on top of the other, implying they also share the same age. To illustrate this fact, three isochrones are shown, for ages of 6,7, and 8×10^8 yr, extracted from the PARSEC stellar models (Bressan et al. 2012) of solar metallicity. The fit supports an age around 70 Myr for both the clusters.

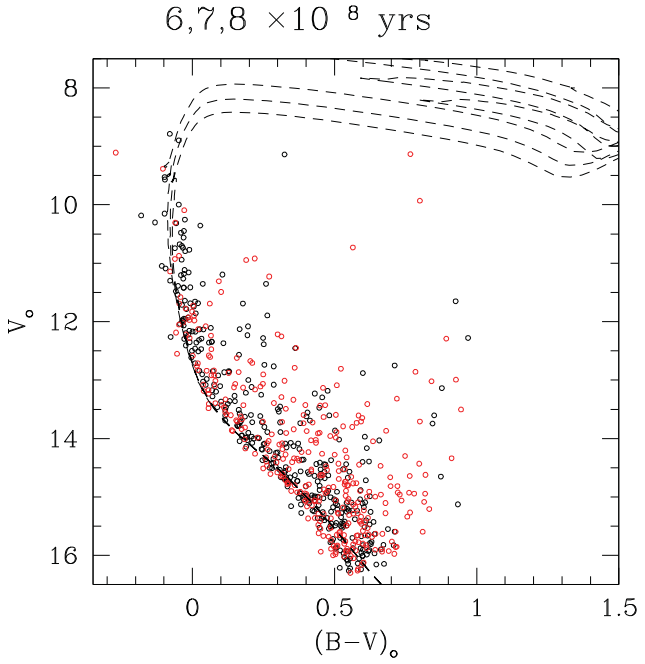

Figure 2. Isochrone solution for NGC 5617 (black symbols) and Trumpler 22 (red symbols) stars. Isochrones are for ages of 60,70, and 80 million years, as indicated in the top of the figure.

3 RADIAL VELOCITIES

Spectra were collected on the 3.9 m Anglo-Australian Telescope (AAT) using the UCLES spectrograph (Diego et al. 1990) and using the HERMES multi-object spectrograph (Sheinis et al. 2014) under service observation time. Summary of the spectroscopic observations are given in Table 2. The star ID numbers for UCLES data are from Haug (1978) for NGC 5617 and from Lindoff (1968) for Trumpler 22. The star ID numbers for HERMES data are from the photometry discussed in Section 2 above.

With UCLES, we obtained spectra over 2012 March 5–6 for six bright cluster stars with a resolution of $R \sim 30\,000$ covering a wavelength range from ∼4550 to ∼7200 Å, using the 31 l mm^{-1}

Table 2. Spectroscopic observations.

Cluster	ID	R.A.	Dec	V	$B-V$	RV ($\mathrm{km\,s^{-1}}$)
			UCLES			
Trumpler 22	32	14 31 29.8	−61 09 28.2	10.50	1.57	− 37.33
Trumpler 22	11	14 31 09.5	−61 09 43.0	10.7	1.30	− 38.96
Trumpler 22	49	14 30 28.7	−61 12 38.8	10.90	1.61	− 40.58
NGC 5617	283	14 30 03.6	−60 50 58.6	8.81	1.22	− 29.55
NGC 5617	116	14 29 28.9	−60 42 18.90	10.67	1.75	− 36.85
NGC 5617	227	14 29 50.5	−60 41 13.1	10.42	1.64	− 35.20
			HERMES			
Trumpler 22	1145	14 31 02.35	−61 06 30.48	13.45	0.46	− 54.42
Trumpler 22	911	14 31 15.73	−61 07 22.16	13.63	0.50	− 34.44
Trumpler 22	983	14 31 11.17	−61 09 11.95	12.69	0.37	− 39.03
Trumpler 22	1079	14 31 05.77	−61 07 29.24	13.38	0.45	− 39.10
Trumpler 22	1327	14 30 52.44	−61 07 11.06	14.00	0.81	− 1.62
Trumpler 22	989	14 31 10.60	−61 05 41.31	13.04	0.55	− 26.75
Trumpler 22	838	14 31 20.21	−61 10 15.60	13.48	0.44	− 39.97
Trumpler 22	799	14 31 22.16	−61 05 24.99	12.40	1.65	− 11.76
Trumpler 22	1188	14 31 00.53	−61 11 44.39	13.24	0.40	− 37.11
Trumpler 22	1136	14 31 03.06	−61 03 28.81	13.69	0.51	− 33.14
Trumpler 22	1085	14 31 05.47	−61 10 04.24	12.47	0.67	37.92
Trumpler 22	794	14 31 23.27	−61 11 25.25	13.52	0.44	− 38.31
Trumpler 22	1026	14 31 08.89	−61 13 09.48	13.07	0.45	− 38.73
Trumpler 22	1122	14 31 03.77	−61 13 38.16	12.18	0.38	− 39.56
Trumpler 22	1230	14 30 58.09	−61 13 07.24	11.72	0.42	− 39.80
Trumpler 22	1417	14 30 46.59	−61 10 03.73	13.66	1.46	− 24.00
Trumpler 22	1315	14 30 53.23	−61 12 35.99	13.83	0.44	− 39.81
Trumpler 22	1222	14 30 58.45	−61 09 07.34	13.74	0.39	− 38.20
Trumpler 22	1050	14 31 07.20	−61 08 32.12	11.86	0.39	− 39.34
Trumpler 22	1363	14 30 49.42	−61 08 29.30	13.60	0.40	− 38.91
Trumpler 22	1404	14 30 47.00	−61 07 24.17	12.28	1.01	− 36.47
Trumpler 22	1381	14 30 48.36	−61 06 28.04	13.84	1.34	− 41.97
NGC 5617	2517	14 29 38.50	−60 47 16.70	13.68	0.63	− 36.84
NGC 5617	2748	14 29 30.70	−60 42 24.10	13.89	0.38	− 40.99
NGC 5617	2930	14 29 24.70	−60 43 03.50	13.74	0.45	− 39.13
NGC 5617	2498	14 29 38.80	−60 43 40.80	13.86	0.39	− 42.36
NGC 5617	2392	14 29 42.50	−60 45 17.10	11.39	0.34	− 41.84
NGC 5617	2148	14 29 50.00	−60 44 37.10	13.25	0.40	− 39.29
NGC 5617	2950	14 29 24.00	−60 41 49.90	13.18	0.36	− 17.04
NGC 5617	2822	14 29 28.50	−60 44 41.40	12.51	0.36	− 37.65
NGC 5617	2382	14 29 42.80	−60 46 19.70	12.81	0.35	− 38.86
NGC 5617	2699	14 29 32.60	−60 46 33.30	13.04	1.31	− 24.18
NGC 5617	2550	14 29 37.50	−60 41 40.40	13.57	0.40	− 39.68
NGC 5617	2348	14 29 43.70	−60 42 46.80	12.13	0.35	− 38.48
NGC 5617	2180	14 29 48.90	−60 39 27.30	12.81	0.38	− 39.94
NGC 5617	2619	14 29 35.20	−60 38 55.80	13.50	0.43	− 38.17
NGC 5617	2181	14 29 48.70	−60 38 37.60	12.10	0.34	− 36.84
NGC 5617	2078	14 29 51.70	−60 38 08.90	10.08	0.10	− 35.01
NGC 5617	1728	14 30 02.00	−60 40 26.50	13.96	0.55	− 39.07
NGC 5617	1935	14 29 55.50	−60 42 26.40	13.75	0.40	− 39.65
NGC 5617	2191	14 29 48.50	−60 42 58.20	10.96	0.30	− 36.80
NGC 5617	2386	14 29 42.60	−60 41 51.30	12.70	0.31	− 34.19
NGC 5617	1687	14 30 03.60	−60 41 09.90	13.38	0.35	− 43.71
NGC 5617	1720	14 30 02.40	−60 42 20.50	12.48	0.29	− 40.03
NGC 5617	1762	14 30 01.10	−60 45 58.30	11.65	0.36	− 40.54
NGC 5617	1611	14 30 06.10	−60 43 16.90	13.14	0.39	− 38.75
NGC 5617	2202	14 29 48.30	−60 45 57.50	11.71	1.84	− 15.86
NGC 5617	1912	14 29 56.30	−60 44 35.00	10.53	0.71	− 39.37
NGC 5617	2074	14 29 52.00	−60 43 30.30	13.52	0.55	− 36.25
NGC 5617	2135	14 29 50.30	−60 47 27.70	13.63	0.58	− 37.75

Table 3. Cluster radial velocities.

	Trumpler 22	NGC 5716
$\langle RV \rangle \pm$ std (km s^{-1})	-38.46 ± 2.08	-38.63 ± 2.25

grating, the blue-sensitive EEV detector, a slit width of 1.5 arcsec, and two times binning in the spatial direction at a central wavelength of 5600 Å. The typical signal-to-noise ratio at the central wavelength was 100 per pixel. The data were reduced using IRAF standard routines to subtract the bias level, apply a flat-field correction, identify and extract spectra, apply a wavelength calibration, and co-add individual spectra.

With HERMES, we obtained spectra on 2014 August 22 for 50 stars from both clusters at a resolution of $R \sim 28\,000$ covering four wavelength ranges from 4710–4900 Å (blue), 5650–5880 Å (green), 6480–6740 Å (red), and 7580–7890 Å (IR). Note that given the large field of view and multi-object capability of HERMES, a single pointing was sufficient to gather spectra of stars in both clusters. The typical signal to noise of the HERMES spectra were 100 per resolution element. The data were reduced using the 2DFDR[4] automatic data reduction pipeline dedicated to reducing multifibre spectroscopy data.

The radial velocities (RV) for the UCLES spectra were measured using the IRAF[5] *fxcor* package, using a solar reference template. For HERMES spectra, correlating against a solar template produced large errors due to differences in spectral type between the Sun and the cluster sample. Instead, the HERMES spectra were cross correlated against an internal reference spectrum, Trumpler 22 star #1122. Careful manual measurement of the spectral features in star #1122 found it has an RV $= -39.56 \pm 1.11$ km s^{-1}. The derived relative RVs of the remaining HERMES spectra were converted to absolute values by applying the RV of the reference star #1122. Note that of the four channels in HERMES, the IR channel wavelength is contaminated by the atmospheric *A*-band absorption features. For this reason, the IR channel was not used for measuring RVs. The typical uncertainty in the RV measurements across the remaining three HERMES channels is of the order of 1–2 km s^{-1}. The typical uncertainty in RVs for the UCLES spectra are less than 1 km s^{-1}.

The final heliocentric corrected RVs of the cluster stars are given in Table 2. The RV analysis reveals that six stars in Trumper 22 (star #1145, #1327, #989, #799, #1085, and #1417) and four stars in NGC 5617 (star #2950, #2699, #2202, and #283) have different RVs compared to the majority of the cluster sample stars. These stars are most likely to be non-members of the respective clusters and are probably field stars that happen to lie within the field of view (see also Section 4 below). Disregarding these stars, the average RV for both clusters are summarized in Table 3. The two clusters have nearly identical RVs, and the measured velocity dispersion in both clusters are comparable with open cluster dispersions. The measured RV for NGC 5617 sample is in agreement with the measurements of Frinchaboy & Majewski (2008) and Mermilliod et al. (2008), who report RV values between -35.77 and -36.60 km s^{-1}, when taking into account the error budget. We have two stars, #116 and #227, in common with both these studies. The difference between us and Mermilliod et al. (2008) is δRV $= 0.04$ and 0.22 km s^{-1} for these two stars, respectively. The difference between us and Frinchaboy & Majewski (2008) is δRV $= -0.19$ km s^{-1} and 0.52 km s^{-1} for these two stars, respectively. In all cases the difference in RV is well within the errors.

[4] www.aao.gov.au/science/software/2dfdr

[5] IRAF is distributed by the National Optical Astronomy Observatories, which are operated by the Association of Universities for Research in Astronomy, Inc., under cooperative agreement with the National Science Foundation.

Table 4. Stellar parameters.

Cluster	ID	$T_{\rm eff}$	log*g*	ξ	[Fe/H]
Trumpler 22	32	4555	1.6	2.72	−0.15
Trumpler 22	49	4970	2.1	2.78	−0.19
Trumpler 22	1381	4600	1.5	1.35	−0.16
NGC 5617	116	4450	1.2	2.44	−0.20
NGC 5617	2074	5800	3.9	1.20	−0.15

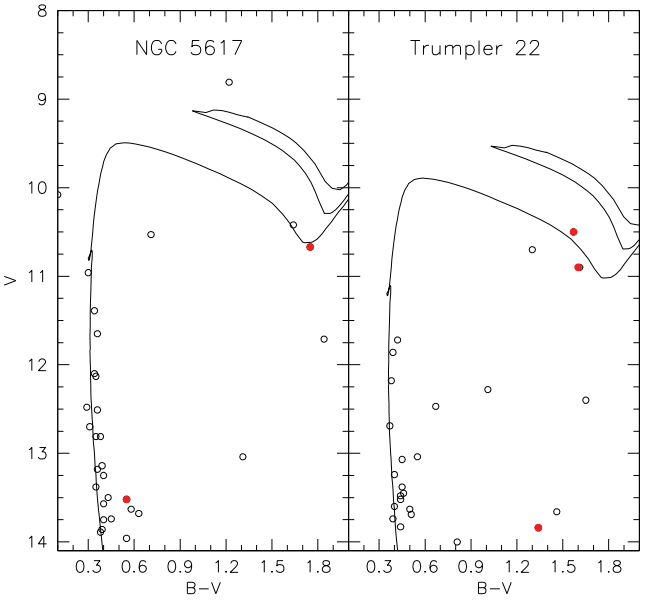

Figure 3. CMD of NGC 5617 and Trumpler 22 for the spectroscopic sample stars, with the stars subject to spectroscopic analysis highlighted in filled red circles. Overlaid is the isochrone for 70 Myr.

4 CHEMICAL ABUNDANCES

Of the total spectra collected, the majority of the targets are either too hot or too fast rotators, such that there are either no measurable spectral line features or all features have been smoothed out. A high fraction of hot stars and rapid rotators are expected in young clusters such as the Trumpler 22 and NGC 5617. Most of the stars that show some measurable spectral features are mostly non-members of the open clusters as determined by the RV analysis.

We carried out a spectroscopic analysis of all RV member stars that displayed a sufficient number of measurable lines, which consists of three stars in Trumpler 22 and three stars in NGC 5617. The spectroscopic sample and their derived stellar parameters are given in Table 4. Their location on the cluster CMD are shown in Fig. 3. Based on its location on the CMD and the derived parameters, Trumpler 22 stars #1381 appears to be a non-member, despite having a similar RV and metallicity as the cluster stars.

For stellar parameters and abundance determinations we use the MOOG code (Sneden 1973) and interpolated Kurucz model atmospheres based on the ATLAS9 code (Castelli, Gratton & Kurucz 1997) with no convective overshooting. The stellar parameter determination procedure was as follows. The equivalent width (EW) of Fe I

Table 5. Chemical abundances.

Cluster	ID	[Na/Fe]	[Mg/Fe]	[Al/Fe]	[Si/Fe]	[Ca/Fe]	[Ni/Fe]
Trumpler 22	32	0.36 ± 0.06	−0.02 ± 0.07	0.02 ± 0.05	0.02 ± 0.07	−0.07 ± 0.05	0.03 ± 0.07
Trumpler 22	49	0.39 ± 0.05	0.09 ± 0.05	0.08 ± 0.06	0.00 ± 0.05	−0.06 ± 0.07	0.06 ± 0.05
Trumpler 22	1381	0.34 ± 0.15	0.05 ± 0.06	0.13 ± 0.10	0.03 ± 0.15	0.03 ± 0.15	0.05 ± 0.11
Average [a]		0.38 ± 0.02	0.04 ± 0.08	0.05 ± 0.04	0.01 ± 0.01	-0.07 ± 0.01	0.05 ± 0.02
NGC 5617	116	0.30 ± 0.07	−0.05 ± 0.06	0.05 ± 0.06	0.05 ± 0.09	−0.03 ± 0.08	0.02 ± 0.08
NGC 5617	2074	0.21 ± 0.04	−0.02 ± 0.05	−0.01 ± 0.05	0.00 ± 0.05	−0.05 ± 0.06	0.01 ± 0.05
Average		0.26 ± 0.06	−0.04 ± 0.02	0.02 ± 0.04	0.03 ± 0.04	−0.04 ± 0.01	0.02 ± 0.01

Note. [a]Average does not include star 1381.

and Fe II lines were measured from the spectra. Estimates of the effective temperature ($T_{\rm eff}$) and log g for each target were made using photometric calibrations of Casagrande et al. (2010) to use as a first guess model. Effective temperature ($T_{\rm eff}$) was derived by requiring excitation equilibrium of the Fe I lines. Microturbulence was derived from the condition that abundances from Fe I lines show no trend with EW. Surface gravity (log g) was derived via ionization equilibrium, i.e. requiring the abundances from Fe I equal Fe II. The number of spectral lines used in the analysis varied due to the difference in wavelength covered by the UCLES and HERMES spectrographs. At minimum 20 Fe I lines and 3 Fe II lines were used in the analysis of HERMES spectra, while the UCLES spectra covered ∼50 Fe I lines and 5–10 Fe II lines. The uncertainty on the derived stellar parameters is of the order of δ $T_{\rm eff}$ = 50 K, δ log g = 0.1 dex, δ microturbulence = 0.1 km s^{-1}, and δ [Fe/H] = 0.1 dex.

Using the derived stellar parameters the abundances for Na, Mg, Al, Si, Ca, and Ni were measured based on line EW measurements. The error on the derived abundances were estimated by quadratically summing the uncertainty in the measured EWs together with the errors due to stellar parameters, which were estimated by varying one parameter at a time, and checking the corresponding variation in the resulting abundances. The total error per star per element is given in Table 5.

The measured abundances find that most elements are in their solar proportions, with the exception of Na. Na abundances are most likely affect by NLTE effects. We make use of the INSPECT web tool at www.inspect-stars.net to determine the impact of NLTE effects on the Na abundances (Lind et al. 2011). We find the NLTE correction is of the order of −0.15 dex, which brings to mean Na abundance in the clusters to slightly above solar level at [Na/Fe] ∼ 0.18 dex.

5 SUMMARY AND CONCLUSIONS

In this paper, we explored the properties of the open cluster NGC 5617 and Trumpler 22. We presented new CCD photometry, from which we find the two clusters share a common age of 70 ± 10 Myr and a common distance of 2.1 ± 0.3 kpc. We examined their RVs based on high-resolution spectra with the AAT-UCLES and AAO-HERMES spectrographs and present RV members of the two clusters. The two clusters share a common average RV of ∼38.5 ± 2.0 km s^{-1}. While the bulk of the spectra collected were either too hot or too fast rotators to carry out spectroscopic analysis, we identified three members in Trumpler 22 and two members in NGC 5617 suitable for chemical analysis. However, star #1381 in Trumpler 22 is most likely to be a non-member based on its position on the CMD, although it has an RV and metallicity similar to that of the cluster members. The abundance results found that both clusters share a common chemical enrichment history with [Fe/H] = −0.18 ± 0.02 dex and no significant differences were seen in the other studied elements between the two clusters within the measurement errors.

The presented evidence is consistent with the two clusters being conatal, confirming that our Galaxy is a host for primordial binary clusters. Further exploration of a larger sample of binary clusters candidates is encouraged to determine the primordial binary cluster fraction within the Galaxy.

ACKNOWLEDGEMENTS

We thank the anonymous referee for helpful suggestions which have improved the paper. GC acknowledges financial support from the AAO Distinguished Visitor programme and ESO DGDF programme during a visit at AAO where part of this work was done. Based on observations obtained at the Anglo-Australian Telescope, Siding Spring Observatory, Australia. We thank the Centre de Données Astronomiques de Strasbourg (CDS), the US Naval Observatory and NASA for the use of their electronic facilities, especially SIMBAD, ViZier and ADS. This paper has made extensive use of the Webda data base at http://www.univie.ac.at/webda.

REFERENCES

Ahumada J. A., 2005, Astron. Nachr., 326, 3
Bastian N., Gieles M., Efremov Y. N., Lamers H. J. G. L. M., 2005, A&A, 443, 79
Bhatia R. K., 1990, PASJ, 42, 757
Bhatia R. K., Hatzidimitriou D., 1988, MNRAS, 230, 215
Bressan A., Marigo P., Girardi L., Salasnich B., Dal Cero C., Rubele S., Nanni A., 2012, MNRAS, 427, 127
Carraro G., 2011, A&A, 536, A101
Carraro G., Munari U., 2004, MNRAS, 347, 625
Carretta E. et al., 2010, ApJ, 722, L1
Casagrande L., Ramírez I., Meléndez J., Bessell M., Asplund M., 2010, A&A, 512, A54
Castelli F., Gratton R. G., Kurucz R. L., 1997, A&A, 318, 841
de la Fuente Marcos R., de la Fuente Marcos C., 2009, ApJ, 700, 436
de la Fuente Marcos R., de la Fuente Marcos C., 2010, ApJ, 719, 104
de Oliveira M. R., Dutra C. M., Bica E., Dottori H., 2000a, A&AS, 146, 57
de Oliveira M. R., Bica E., Dottori H., 2000b, MNRAS, 311, 589
Dieball A., Grebel E. K., 2000, A&A, 358, 897
Dieball A., Müller H., Grebel E. K., 2002, A&A, 391, 547
Diego F., Charalambous A., Fish A. C., Walker D. D., 1990, in Crawford D. L., ed., Proc. SPIE Conf. Ser. Vol. 1235, Instrumentation in Astronomy VII. SPIE, Bellingham, p. 562
Dufton P. L., Brown P. J. F., Fitzsimmons A., Lennon D. J., 1990, A&A, 232, 431
Efremov Y. N., 1995, AJ, 110, 2757

Fall S. M., Chandar R., Whitmore B. C., 2005, ApJ, 631, L133
Frinchaboy P. M., Majewski S. R., 2008, AJ, 136, 118
Fujimoto M., Kumai Y., 1997, AJ, 113, 249
Haug U., 1978, A&AS, 34, 417
Kopchev V. S., Petrov G. T., 2008, Astron. Nachr., 329, 845
Larsen S. S., 2000, MNRAS, 319, 893
Leon S., Bergond G., Vallenari A., 1999, A&A, 344, 450
Lind K., Asplund M., Barklem P. S., Belyaev A. K., 2011, A&A, 528, A103
Lindoff U., 1968, Ark. Astron., 4, 493
Marco A., Bernabeu G., 2001, A&A, 372, 477
Mermilliod J. C., Mayor M., Udry S., 2008, A&A, 485, 303
Minniti D., Rejkuba M., Funes J. G., Kennicutt R. C., Jr, 2004, ApJ, 612, 215
Orsatti A. M., Feinstein C., Vergne M. M., Martínez R. E., Vega E. I., 2010, A&A, 513, A75
Schmidt-Kaler T., 1982, in Schaifers K., Voigt H., eds, Landolt-Brnstein - Group VI Astronomy and Astrophysics, Vol. 2b, Stars and Star Clusters. Springer-Verlag, Berlin, p. 14
Sheinis A. et al., 2014, in Gimi B., Molthen R. C., eds, Proc. SPIE Conf. Ser. Vol. 9147, Medical Imaging 2015: Biomedical Applications in Molecular, Structural, and Functional Imaging. SPIE, Bellingham, p. 91470Y
Sneden C. A., 1973, PhD thesis, Univ. Texas at Austin
Stetson P. B., 1987, PASP, 99, 191
Subramaniam A., Gorti U., Sagar R., Bhatt H. C., 1995, A&A, 302, 86
Uribe A., García-Varela J.-A., Sabogal-Martínez B.-E., Higuera G. M. A., Brieva E., 2002, PASP, 114, 233
Vázquez R. A., Moitinho A., Carraro G., Dias W. S., 2010, A&A, 511, A38
Whitmore B. C. et al., 2005, AJ, 130, 2104

SUPPORTING INFORMATION

Additional Supporting Information may be found in the online version of this paper:

Appendix A. Atomic line list (http://mnras.oxfordjournals.org/lookup/suppl/doi:10.1093/mnras/stv1583/-/DC1).

Please note: Oxford University Press are not responsible for the content or functionality of any supporting materials supplied by the authors. Any queries (other than missing material) should be directed to the corresponding author for the paper.

APPENDIX A: ATOMIC LINE LIST

The full table of atomic line data is available online.

Element	Wavelength (Å)	LEP (eV)	log *gf*	EW (mÅ)
		Trumpler 22: #32		
Fe I	4808.15	3.25	−2.79	89
Fe I	5067.15	4.22	−0.97	153
Fe I	5217.39	3.21	−1.07	192
Fe I	5285.13	4.43	−1.64	86
Fe I	5322.04	2.28	−2.8	188
Fe I	5373.71	4.47	−0.76	132

This paper has been typeset from a TEX/LATEX file prepared by the author.